

ESR spectroscopic evidence for hydration- and temperature-dependent spatial perturbations of a higher plant cell wall paramagnetic ion lattice

To study the influence of cell wall polyuronide structure on bound paramagnetic ion interactions, spin-spin coupling measurements were made on intact cell walls exchanged with a wide range of Mn^{2+} and Cu^{2+} concentrations. These experiments were performed so that dimer-only intercationic nearest neighbor distances (d) and lattice constants (κ) could be calculated from the linewidth-concentration dependency. d values were estimated to be 12 and 14 Å for Cu^{2+} and Mn^{2+} , respectively. At the maximal bound ion concentration, κ was 2.3–2.6, indicating that about 5–7 paramagnetic ion nearest neighbor spin-spin interactions occur per dipole in the nearly filled lattice. This latter observation strongly argues for the egg-box model of the cell wall-polyuronide lattice structure. Mn^{2+} linewidths of hydrated cell wall-bound paramagnetic ions displayed an unusual temperature dependency, whereby linewidths increased between 20°C and the temperature at which maximal linewidths were observed (T_{max}). T_{max} was inversely proportional to the degree of lattice hydration, indicating that the temperature dependency was not associated with the freezing of bound water. The relative change in Mn^{2+} linewidths, between 20°C and T_{max} , was affected by binding site-associated ^1H spin-lattice relaxation times, indicating that the temperature dependency is at least partially controlled by cell wall polyuronide structure.

Introduction

The primary cell wall/middle lamellar complex of higher plant tissues [1] is considered to be a three-phase system consisting of a 'crystalline' component (cellulose), a 'matrix' component (one of which is uronic acid-containing polymers), and a bound water or 'packing' component which can take up to about 50% (w/w) of the total primary wall complex mass. Of the matrix components,

galacturonic acid-containing polymers are one of the most important because of their involvement in stabilizing the wall structure [1–4], controlling the ion exchange capabilities of the apoplast [2,5], and exerting conformational or steric control over the activity of certain hydrolytic enzymes [2,3]. Much needs to be learned about the relationship between changes in ionic polymer matrix structure and the microscopic properties of the primary wall and middle lamellae during plant growth and development, since the various lattice interactions control many of the bulk physical properties of tissues.

In previous studies [6], we presented direct evidence that the divalent cationic binding mechanism in plant cell walls was sequential and pro-

* To whom correspondence should be addressed.

** Present address: Department of Chemistry, Oakland University, Rochester, MI 48063, U.S.A.

*** Agricultural Research Service, U.S. Department of Agriculture.

Abbreviation: PGA, polygalacturonic acid.

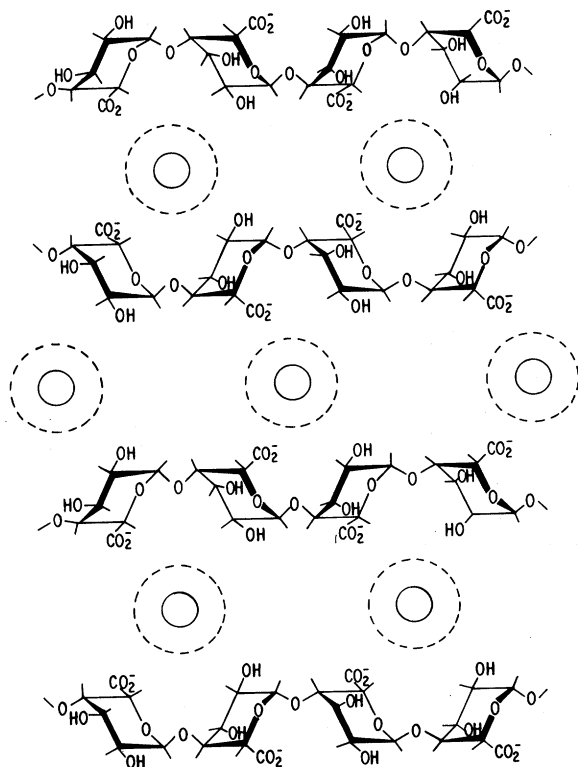


Fig. 1. Egg-box model [7-11] for the polyuronide-divalent cation aggregate structure. Broken circles represent one aquoshell. The intercationic distances are drawn to be on the order of 12 Å. From this two-dimensional lattice model, the lattice constant (κ) for spin-spin coupling, for the center ion, is about 2.45. In a three-dimensional model, κ would increase up to 3.88, depending on the relative position of the upper and lower planes in relation to the center paramagnetic ion; spin-spin couplings 20 Å or more cause very little line broadening and therefore can be neglected.

posed that the ion-polyuronide structure was similar to the egg-box model hypothesized previously [7-11]; in this model, the metal ions are chelated between adjacent polymer chains (Fig. 1) in an ordered fashion by negatively charged carboxyl groups. In this report, we present data which further support this binding mechanism and lattice model. We also present evidence that the cell wall complex polyuronides undergo heretofore unknown hydration- and temperature-dependent conformational alterations. The ESR technique we discuss could be a useful research tool to further elucidate the structural mechanisms of various cell wall polyuronide-mediated processes, since devel-

opmental changes in plant tissues are regulated to some degree by the organization and conformation of these acid sugar polymers [1-4].

Materials and Methods

Intact cortical tissues of *Malus pumila* fruit were used throughout the experiments reported in this study. Tissue fixation and determination of free uronic acid concentrations were described before [6]. Cross polarization and magic angle spinning NMR (CPMAS NMR) experiments on tissues with different binding site-associated ^1H spin-lattice relaxation times ($\text{C}=\text{O } T_{1\text{H}}$) were as previously described [12].

For the ESR experiments, intact tissues ($1 \times 1 \times 4$ mm) were equilibrated at pH 5 in water for 15 min and decanted; this procedure was repeated thrice. Approx. 10-40 mg (dry weight) of cell wall complex was used for each treatment combination depending on the concentration of bound ion. Samples were equilibrated ($22 \pm 2^\circ\text{C}$) in 10 ml of various concentrations of Mn^{2+} and H^+ (10^{-3} - 10^{-1} M, pH 2-5) in order to achieve a wide range of bound paramagnetic ion concentrations. For Cu^{2+} experiments, cell wall samples were equilibrated (pH 4.5) in 10^{-6} - 10^{-2} M aqueous CuCl_2 . After approx. 24 h, the solutions were decanted and the tissue specimens washed thrice in (pH 7) water, allowing 15 min equilibration in each wash. After an additional 1 h soak in water, this procedure was repeated. Samples were dehydrated with ethanol and critical point dried as previously described [6,12].

In order to achieve different levels of hydration (21.7 ± 0.3 , 32.9 ± 0.5 , 42.0 ± 0.4 and $51.7 \pm 0.5\%$ (w/w)) samples were equilibrated for various time intervals (0.5-0.75, 1-1.5, 2-3, and 4-6 h, respectively) in a saturated water vapor chamber at 160 torr and 22°C . Determination of bound water was performed gravimetrically by difference, before and after equilibration. Bound water levels never exceeded 50-75% (w/w) after equilibrium hydration. Hydrated samples were immediately loaded and sealed in 3×130 mm quartz tubes, and spectra were taken proceeding from the high temperature treatments first (20°C). After each experiment, the samples were removed, washed in methanol, vacuum dried at 35°C , weighed, and

dry ashed for atomic absorption spectrophotometric analysis of Mn and Cu using standard procedures. Specific departures from or additions to these experimental methods are given in figure and table headings.

Mn²⁺ ESR spectral parameters, linewidths ($\Delta H_{(dI(H)/dH)_{\max}}$) and nearest neighbor distance parameter (d) calculations were as previously described [6]. Cu²⁺ linewidths were calculated directly from the first derivative g_{\perp} component as the difference in field strength (expressed in G) between the maximum and minimum amplitude with: scan range, 1.6 kG; field set, 3 kG; modulation amplitude, 4 G; microwave frequency, 9.1 GHz; microwave power, 20.75 dB; scan times, 4–32 min depending on concentration and gain levels; time constants, 0.032–0.256 s on a Varian Series E-109B * spectrometer at -180°C . This measure of linewidth is directly proportional to the true linewidth as determined by an anisotropic simulation routine [13]; this simulation showed that the true Cu²⁺ linewidth ($\Delta H_{(dI(H)/dH)_{\max}}$, Fig. 3) is equal to the empirical measure, described above, divided by 1.17.

In Table I, ΔT_{\max} is the change in temperature, relative to the 22% (w/w) level of hydration, when $\delta\Delta H_{(dI(H)/dH)_{\max}}/\delta T = 0$. For these data alone, all linewidth data (320 observations encompassing all hydration levels, temperatures, $[\text{Mn}^{2+}]_{\text{bound}}$ and $T_{1\text{H}}$) were fit to a statistical model quadratic in $[\text{Mn}^{2+}]_{\text{bound}}$ and temperature (T). The partial first derivatives were taken with respect to T and $[\text{Mn}^{2+}]_{\text{bound}}$ and set to zero such that:

$$\delta\Delta H_{(dI(H)/dH)_{\max}}/\delta T = 0; a_1T + b_1[\text{Mn}^{2+}]_{\text{bound}} = C_1$$

and

$$\delta\Delta H_{(dI(H)/dH)_{\max}}/\delta[\text{Mn}^{2+}]_{\text{bound}} = 0;$$

$$a_2T + b_2[\text{Mn}^{2+}]_{\text{bound}} = C_2$$

T_{\max} values were calculated by the method of simultaneous equations whereby:

$$T_{\max} = \frac{a_1b_1}{c_2b_2} \div \frac{a_1b_1}{a_2b_2}$$

Polygalacturonic acid (H⁺ form, PGA) was purchased from Sigma Chemical Company (Lot: 112F-0303), St. Louis, MO, U.S.A. About 500 mg PGA was equilibrated in 25 ml of 800, 400, 100, 50 and 2 mM CaCl₂ in 75% (v/v) ethanol/water to achieve 53 ± 4 , 38 ± 2 , 25 ± 8 , 11 ± 2 and $0.3 \pm 0.03\%$ (on a binding site basis whereupon one site equals 2CO₂⁻) bound Ca²⁺, respectively. Samples were washed repeatedly with absolute ethanol, vacuum dried on sintered glass, and stored under vacuum (160 torr) over dehydrated silica gel for 2–3 weeks prior to the CPMAS NMR experiments.

Values of $T_{1\text{H}}$ were determined indirectly via observation of ¹³C magnetization after ¹H-¹³C polarization transfer (0.8 ms) in a 180°-τ-90° pulse sequence (τ, variable time delay). Recycling times were approx. 1.5 s. Each spectrum required an accumulation of 4000 transients. For determination of ¹H-¹³C polarization transfer rates (T_{CH}^{-1}), carbonyl carbon (C=O) and nonspecific ring carbon (COH) resonance intensities were measured after accumulation of 4000 scans with variable cross polarization times of 0.050–0.8 ms. ¹³C signal amplitudes were plotted as a function of the variable delay or cross polarization times, and data were treated by standard literature methods. Standard errors were calculated from the least-squares analysis of all $T_{1\text{H}}$ and T_{CH} data. All CPMAS NMR experiments were performed in the presence of dry N₂ flow.

Results and Discussion

In fluids, rapidly tumbling averages the angular component of the spin-spin dipolar coupling Hamiltonian to zero [14]; however, in randomly oriented solid matrices [15], both the interactions between nearest neighbor paramagnetic ions and the coupling of the bound ions with the thermal motions of the surroundings need to be considered. From the standpoint of linewidths alone, the latter term has a small effect relative to the interactions between the ions themselves [15] and, thus, bound paramagnetic ions can be considered as fixed points interacting only through their cou-

* Reference to brand or firm name does not constitute endorsement by the U.S. Department of Agriculture over others of a similar nature not mentioned.

pling with each other. Because of this simplified picture, the i th spin in the midst of other paramagnetic ions bound within a solid, such as a nearly filled idealized cell wall lattice, has a total interaction profile equal to the sum of the dipolar coupling terms (spin-spin and/or exchange) over all j th interactions. In this summation [15], the series converges to some value which depends only on those dipoles in the vicinity of each i th spin and, therefore, is the same for all the dipoles of the same type in the lattice. Only spins on the lattice surface would experience relatively fewer j th interactions. Of the dipolar terms, spin-spin coupling causes line broadening [16] and falls off as the inverse cube of the distance between interacting spins [15–19] as described [16,23] by the square root of the second moment of a Gaussian line. In nonmagnetic insulators [20], linewidths and shapes agree with basic Van Vleck theory [16]. However, as paramagnetic ions or molecules become very close (for example, on the order of 5 Å [16]) to each other [18], the observed linewidths are affected by exchange [21] coupling which determines the rate that dipolar fields fluctuate in time [22] and is dependent upon the ‘bonding pathway’ between two spin systems [17]. While second moments are independent of the exchange term [22], the lineshapes no longer remain Gaussian and become mixed [23]. Because of this, one observes line narrowing [16,21,24,25] in the spectra.

Since the linewidths of Mn^{2+} , intercalated in a higher plant cell wall matrix, only increased as a function of bound ion concentration and decreased with nonparamagnetic divalent cation doping, we felt that little or no exchange narrowing occurred [6]; however, only a limited concentration range was utilized. Further evidence is presented in Figs. 2 and 3 for both Mn^{2+} and Cu^{2+} , respectively. The fact that the linewidths for cell wall-bound Mn^{2+} and Cu^{2+} only increase as a function of paramagnetic ion concentration argues strongly against any significant exchange coupling and, therefore, we can neglect this contribution to linewidth. We approximate a dimer-only nearest neighbor distance parameter (d) from the extrapolated zero concentration-linewidth intercept. This near dilute limit calculation gives the most reliable results when utilizing Van Vleck theory

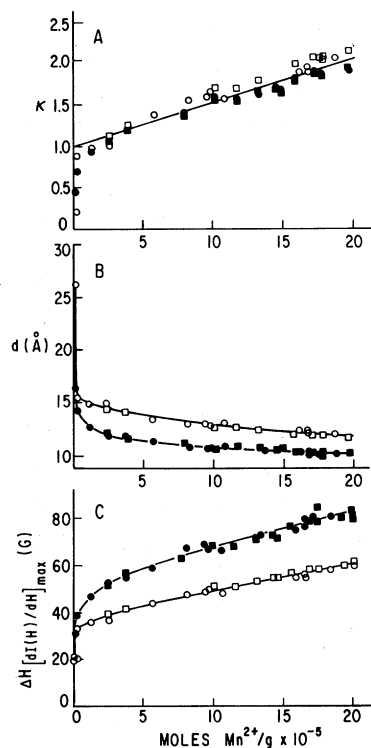


Fig. 2. Cell wall-bound Mn^{2+} concentration ($\times 10^{-5}$ mol/g) dependency of linewidth ($\Delta H_{(dI(H)/dH)_{\max}}$), dilute limit nearest neighbor distance parameters (d , assuming $\kappa = 1$) and lattice constants (κ). Open symbols are equilibrium hydrated; closed symbols are critical point dried. Squares and circles represent two independent experiments. The d values used to calculate κ were 13.72 and 16.3 Å for dry and hydrated tissues, respectively. ESR spectra were taken with a sample temperature of -180°C .

[16]. Using this approach, the dimer paramagnetic ion nearest neighbor distances were estimated to be 12 and 14 Å (dehydrated samples) for Cu^{2+} and Mn^{2+} , respectively. At these distances, which are close to the intercationic distances of the egg-box structure [7,26,27] depicted in Fig. 1, little exchange narrowing should occur for noncovalently bound paramagnetic species. The difference in d between Mn^{2+} and Cu^{2+} samples could be due to the fact that Cu^{2+} loses a significant portion of its aquoshell [28,29], unlike other transition ions, such as Mn^{2+} , and might result in a more compact paramagnetic lattice structure. In Figs. 2 and 3, the dimer-only nearest neighbor distance parameter d is presented as a function of the concentration of bound metal ion. These calcula-

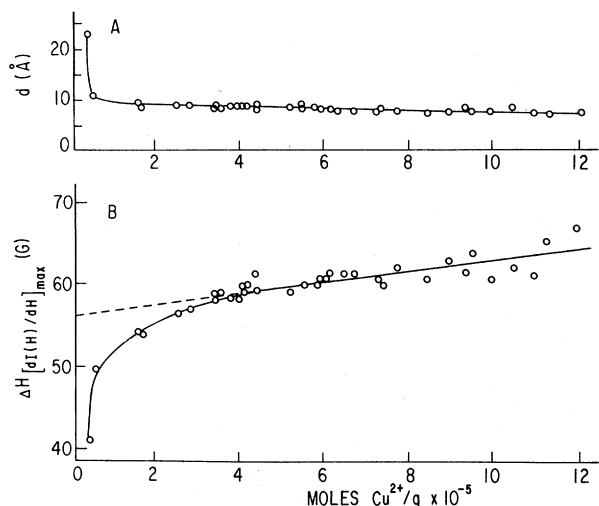


Fig. 3. Cu^{2+} linewidth ($\Delta H_{(dI(H)/dH)_{\max}}$) and dilute limit nearest neighbor distance parameters (d) dependency on cell wall-bound Cu^{2+} ($\times 10^{-5}$ mol/g) at -180°C . This calculation for d assumes $\kappa = 1$ throughout. Samples were dehydrated. The dilute limit Cu^{2+} linewidth intercept (dotted line) is approx. 56 G.

tions assume that $\kappa = 1$ in the relation:

$$\Delta \Delta H_{(dI(H)/dH)_{\max}} = 28690 \cdot \text{G} \cdot \text{\AA}^3 \cdot [S(S+1)]^{1/2} \kappa / d^3$$

where κ is the lattice constant, d is the nearest neighbor distance and S is the total spin [6,18,19]. In fact, the change in line-broadening ($\Delta \Delta H_{(dI(H)/dH)_{\max}}$) cannot be attributed solely to a change in d ; for as ions fill the lattice, an increase in the number of interactions per ion will occur. For example, in the very dilute limit no nearest neighbor interactions will be expected, whereas up to 12 nearest neighbor interactions will be found in a filled lattice. κ varies with the lattice structure as well as the degree of filling. Considering nearest neighbor interactions only, $\kappa = 1$ for a dimer, 1.4 for a linear array, 2.45 for a two-dimensional hexagonal array with six nearest neighbors as in Fig. 1, and 3.46 for a three-dimensional hexagonal close packing array (12 nearest neighbors). In this simplified example, κ^2 gives the number of nearest neighbors; however, even for a system with an extended array, due to the decreased weighting of distant interactions, κ^2 will approximate the number of nearest neighbors. Fig. 2A shows calculated lattice constants (κ), assum-

ing a constant d . The dilute limit asymptote is set to unity (dimer interactions only). As expected for the sequential ion-binding model, κ approaches zero only at a very low concentration (e.g., less than 1% of the available sites being filled or approx. $2 \cdot 10^{-6}$ mol Mn^{2+} /g cell wall), where a significant portion of the i th dipoles experience no interactions with neighboring spins. From this linear relationship (Fig. 2A), we calculated that the maximum κ value is approx. 2.45 ± 0.21 for Mn^{2+} and Cu^{2+} , which indicates that the average number of spin-spin interactions per i th dipole is in the order of 5–7 (κ^2), assuming the intercationic distances in the lattice are about equal, and argues strongly for the sequential divalent cation-binding [6] egg-box model [7–11] of a filled lattice. The maximum value of 2.45 found in this work is lower than that expected for a filled three-dimensional array. However, this is not surprising since approx. 50% [12] of the total uronic acid polymers in this system are methylated and therefore bind no divalent cations. Indeed, the observed value of κ_{\max} argues for the existence of pockets or regions of nonmethylated polymer existing contiguously in the cell wall/middle lamella lattice.

Upon equilibrium hydration (Fig. 2B and C, open symbols), the dimer-only Mn^{2+} nearest neighbor distance parameter increases about 2 Å (10 G decrease in $\Delta H_{(dI(H)/dH)_{\max}}$ as $[\text{Mn}^{2+}]_{\text{bound}}$ approaches zero). This linewidth change is not likely to be due to the hydration of the transition ions alone, since the difference in water adsorption after equilibrium hydration between ionically concentrated and dilute samples is within experimental error (0.44 ± 0.02 g water/g cell wall) and because bound divalent cations, such as Mn^{2+} , have a rather significant hydration shell even in the dehydrated state. This latter point is demonstrated (Fig. 4) by experiments on the spin-lattice relaxation time (T_{1H}) and cross polarization transfer rates (T_{CH}^{-1}) of pure, dry Ca^{2+} salts of polygalacturonic acid (Ca^{2+} PGA) via CPMAS NMR. In solids, spin-lattice relaxation is mediated by ^1H spin diffusion [30] such that in homogeneous samples with rapidly reorienting ^1H -rich domains such as methyl groups or bound water, polymer T_{1H} values will be inversely proportional to the molar concentration of these domains [31]. This phenomenon is clearly established in Fig. 4, wherein poly-

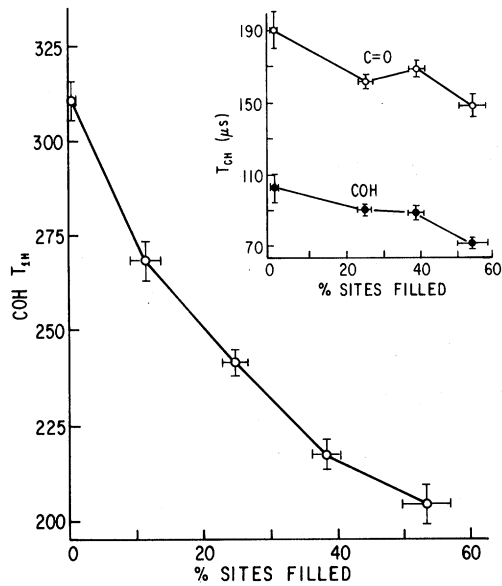


Fig. 4. ^1H spin-lattice ($T_{1\text{H}}$) and cross polarization (T_{CH}) relaxation times of dehydrated polygalacturonate as a function of bound Ca^{2+} . Bars represent standard errors of the means ($[\text{Ca}^{2+}]_{\text{bound}}$) or asymptotic standard error (relaxation times).

uronide $T_{1\text{H}}$ values decline as the binding sites become filled with Ca^{2+} . If ionically associated bound water were not present, one would expect either no change in $T_{1\text{H}}$ or an increase due to the cross-linking effect of Ca^{2+} on PGA motion. Other evidence for the existence of a significant amount of bound water in 'dry' polymer salts is demonstrated (Fig. 4, insert) by the decrease in remotely protonated ^{13}C signal (C=O) T_{CH} values as the anionic polymer lattice becomes increasingly populated with Ca^{2+} . The cross polarization rate (T_{CH}^{-1}) of ^{13}C resonances with directly bonded protons (for example, the ring carbons [COH] of Ca^{2+} PGA) is a function of the inverse 6th power of the distance between ^{13}C and ^1H spins [32]. For this reason, carboxylate functionality (C=O) T_{CH} values are larger [33] than corresponding ring carbon values. The greater relative effect of bound Ca^{2+} on C=O T_{CH} (36% greater negative slope) is evidence that the bound water protons are closer to the carboxylate groups, as would be expected for the ionic lattice we propose (Fig. 1, and Ref. 6). Since dehydrated divalent cation-polyuronide lattices show significant cation aquoshells, we propose that the 2 Å difference in dilute limit d values is due to changes in the anionic polymer

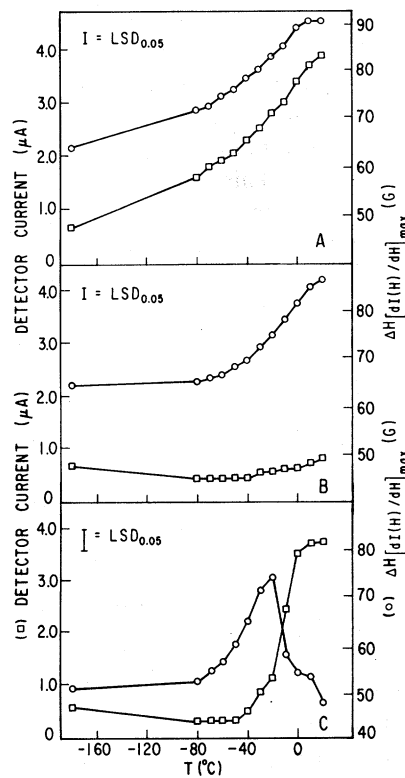


Fig. 5. Temperature dependence of cell wall-bound Mn^{2+} linewidths ($\Delta H_{(dI(H)/dH)_{\text{max}}}$, $^{\circ}$) and ESR detector current ($\times 10^2 \mu\text{A}$, \square) for methanol-treated (A), slightly hydrated (approx. 8% (w/w), B), and equilibrium hydrated (approx. 70% (w/w), C). Tissue specimens had ca. $1.89 \cdot 10^{-5}$ mol Mn^{2+} /g cell wall (approx. 6% of the available sites filled). Least significant differences at the 0.05 level ($\text{LSD}_{0.05}$) are reported for each figure. Data are the means of three experiments.

conformation upon equilibrium hydration.

In order to further elucidate the mechanism of the hydration effect, we performed experiments on Mn^{2+} spin-spin coupling as a function of sample temperature (20 to -180°C) for slightly hydrated (approx. 8% (w/w), Fig. 5B), equilibrium-hydrated (Fig. 5C), and methanol-treated (Fig. 5A) samples ($[\text{Mn}^{2+}]_{\text{bound}} = 1.9 \cdot 10^{-5}$ mol/g cell wall or 6% of the binding sites being filled). The methanol and 8% hydrated cell wall complexes displayed a similar temperature response between 20 and -180°C , albeit the rate of change in linewidth for the methanol-treated samples was more gradual. The equilibrium hydrated samples had an unusual temperature dependency, whereupon the 20 and -180°C linewidths were approximately equal but

bound paramagnetic ion linewidths increased between 20°C and T_{\max} , where the maximum linewidth was observed. The spin-spin coupling maximum was associated with a sharp decline in spectrometer detector current (350–100 μA) over a narrow temperature range. This latter result might indicate that the observed maximum linewidth at T_{\max} was due to a polymer phase change upon the freezing of bound water (for example, whereupon the sample dielectric constant drops and thereby reduces the observed detector current). Assuming a constant κ , the relative change in linewidth between 20°C and T_{\max} (Fig. 5C) would indicate a decrease in the Mn^{2+} nearest neighbor distance parameter (Δd) of about 2.6 Å. Other investigators [34] have found that paramagnetic crystals show little linewidth variation between 27 and –100°C; at lower temperatures (–100 to –171°C), a crystalline phase change coincided with paramagnetic ion spectral narrowing. Thus, our observed temperature-dependent changes in Mn^{2+} linewidths could be associated with alterations in the cation-binding polymer conformation. If the bound paramagnetic ion spin-spin interaction increase, between 20°C and T_{\max} , is associated with a polyuronide water of hydration phase change upon freezing, T_{\max} should decrease as the degree of sample hydration is lowered; this was not observed upon further investigation (Fig. 6).

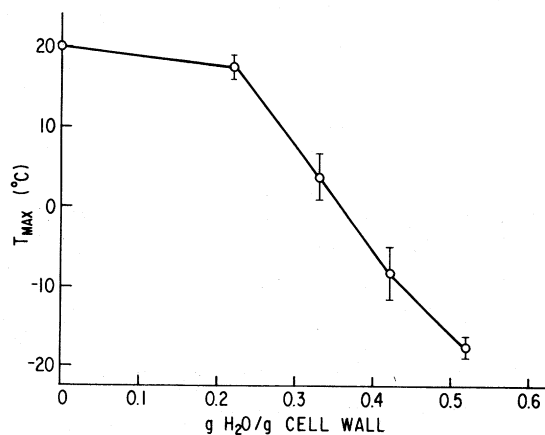


Fig. 6. Dependency of T_{\max} (temperature where maximum linewidths were observed) on of lattice hydration. Each data point is the mean of four replications ($[\text{Mn}^{2+}]_{\text{bound}}$ varied between ca. $1 \cdot 10^{-4}$ and $3 \cdot 10^{-4}$ mol/g or approx. 32 and 95% available sites filled). Bars represent two standard errors of each mean.

TABLE I

DEPENDENCE OF ΔT_{\max} AND Δd ON THE HYDRATION OF THE CELL WALL LATTICE AS A FUNCTION OF BINDING SITE-ASSOCIATED ^1H SPIN-LATTICE RELAXATION TIMES ($\text{C}=\text{O } T_{1\text{H}}$)

Samples with differing $\text{C}=\text{O } T_{1\text{H}}$ values had virtually identical levels of bound divalent cations ($1.26 \cdot 10^{-5} \pm 6.32 \cdot 10^{-7}$ mol/g) and degree of methyl esterification [12], either of which can act as a ^1H relaxation agent via water of hydration (Fig. 4) or methyl rotation [31], respectively. Thus, carboxylate functionality $T_{1\text{H}}$ data [12] probably reflect differences in uronic acid polymer size. Relaxation times, all complicating factors being equal, are inversely related to solid polymer motion [30]. ΔT_{\max} is the change in temperature, relative to the 22% (w/w) level of hydration, when $\delta\Delta H_{(dI(H)/dH)_{\max}}/\delta T = 0$. For the ΔT_{\max} column alone, all linewidth data (320 observations encompassing all hydration levels, T , $[\text{Mn}^{2+}]_{\text{bound}}$ and $T_{1\text{H}}$) were fit to a statistical model quadratic in $[\text{Mn}^{2+}]_{\text{bound}}$ and T . The partial first derivatives were taken with respect to T and $[\text{Mn}^{2+}]_{\text{bound}}$ and set to zero. T_{\max} values were calculated by the method of simultaneous equations. The statistical model also predicts a significant inverse relationship between T_{\max} and $[\text{Mn}^{2+}]_{\text{bound}}$. Δd is the calculated change in the Mn^{2+} nearest neighbor distance parameter between 20°C and T_{\max} assuming $\kappa = 2.5$ and that all linewidth changes are due to distance effects; of course paramagnetic ion T_1 values are expected to change with T and this may have a substantial contribution to the observed linewidth changes. Only samples which had a narrow $[\text{Mn}^{2+}]_{\text{bound}}$ range ($3.1 \cdot 10^{-4} \pm 3.9 \cdot 10^{-6}$ moles/g or 94 \pm 1% sites filled, \pm S.E.) were used for this calculation. Δd values were calculated from the observed data without a priori curve fitting.

$\text{C}=\text{O } T_{1\text{H}}$ (ms)	g H ₂ O/g cell wall	ΔT_{\max} (Cdeg)	Δd (Å)
333 \pm 12	0.22	0	0.1
	0.33	-10	0.2
	0.42	-20	0.6
	0.52	-29	1.9
123 \pm 15	0.22	0	0.1
	0.33	-5	0.5
	0.42	-14	1.5
	0.52	-23	2.7

Indeed, as sample hydration was raised from approx. 20 to 50% (w/w), the T_{\max} declined linearly (four replications with $[\text{Mn}^{2+}]_{\text{bound}}$ ranging between approx. $1 \cdot 10^{-4}$ to $3 \cdot 10^{-4}$ mol/g cell wall). The average T_{\max} was above 0°C in all but two of the samples. From these data, we conclude that the linewidth-temperature dependency was not directly related to the freezing of bound water.

In order to test the hypothesis that the change in cell wall-bound Mn^{2+} linewidths between 20°C

and T_{\max} was associated with ligand structure, we utilized samples differing in binding site-associated (C=O) ^1H spin-lattice relaxation times [12] (Table I). In both samples the changes in T_{\max} (ΔT_{\max}), relative to the lowest level of hydration, were approximately equal. However, the total change in Mn^{2+} linewidths between 20°C and T_{\max} , as reflected in the nearest neighbor distance parameter (Δd), was significantly larger in the equilibrium hydrated cell wall samples with short C=O $T_{1\text{H}}$ values and indicates a greater degree of lattice flexibility. All these experiments argue that the temperature dependency is related to changes in cell wall polyuronide spatial orientation. Because of the relative sensitivity of this ESR technique, it could be used to study structural alterations of paramagnetic ion or nitroxide-labeled polymers in such mechanistically obscure plant developmental processes as extensive growth, polymer deposition and orientation with respect to the longitudinal wall axis.

From these and other [6] studies, we conclude that divalent cations bind within the cell wall/middle lamellar complex in a spatially sequential fashion, that the ion-polyuronide aggregate structure is similar to that proposed for polyuronides in solution [9] and that the free acid polymers exist in three-dimensional lattices low in methyl ester content. The hydrated ionic lattice shows an unusual temperature-dependent perturbation of paramagnetic ion spin-spin coupling. Other data indicate that the relative position of the fixed dipoles decrease 2–3 Å on dehydration probably under the influence of spatial alterations in the conformation and structure of the anionic ligand.

Acknowledgments

We would like to thank Drs. J.J. Shieh, P.E. Pfeffer and J. Phillips for use of the ESR spectrometer, CPMAS NMR, and statistical analyses, respectively.

References

- Hall, M.A. (1981) Quality in Stored and Processed Vegetables and Fruits, pp. 53–64, Academic Press, London
- Demarty, M., Morvan, C. and Thellier, M. (1984) *Plant Cell Environ.* 7, 441–448
- Ferguson, I.B. (1984) *Plant Cell Environ.* 7, 477–489
- Tepper, M. and Taylor, J.E.P. (1981) *Can. J. Bot.* 59, 1522–1525
- Van Cusem, P. and Gillet, C. (1982) *J. Exp. Bot.* 33, 847–853
- Irwin, P., Sevilla, M. and Shieh, J. (1984) *Biochim. Biophys. Acta* 805, 186–190
- Gidley, M.J., Morris, E.R., Murray, E.J., Powell, D.A. and Rees, D.A. (1979) *J. Chem. Soc. Chem. Commun.* 1979, 990–992
- Gidley, M.J., Morris, E.R., Murray, E.J., Powell, D.A. and Rees, D.A. (1980) *Int. J. Biol. Macromol.* 2, 332–334
- Grant, G.T., Morris, E.R., Rees, D.A., Smith, P.J.D. and Thom, D. (1973) *FEBS Lett.* 32, 195–198
- Morris, E.R., Powell, D.A., Gidley, M.J. and Rees, D.A. (1982) *J. Mol. Biol.* 155, 507–516
- Thom, D., Grant, G.T., Morris, E.R. and Rees, D.A. (1983) *Carbohydr. Res.* 100, 29–42
- Irwin, P., Pfeffer, P., Gerasimowicz, W., Pressey, R. and Sams, C. (1984) *Phytochem.* 23, 2239–2242
- Lefebvre, R. and Maruani, J. (1965) *J. Chem. Phys.* 42, 1480–1496
- Eaton, S.S., More, K.M., Sawant, B.M., Boymel, P.M. and Eaton, G.R. (1983) *J. Mag. Reson.* 52, 435–449
- Pryce, M.H.L. and Stevens, K.W.H. (1950) *Proc. Phys. Soc. (Lond.)* A63, 36–51
- Shinar, J. and Jaccarino, V. (1983) *Phys. Lett.* 91A, 132–134
- Damoder, R., More, K.M., Eaton, G.R. and Eaton, S.S. (1984) *Inorg. Chem.* 23, 1320–1326
- Eaton, S.S., More, K.M., Sawant, B.M. and Eaton, G.R. (1983) *J. Am. Chem. Soc.* 105, 6560–6566
- Van Vleck, J.H. (1948) *Phys. Rev.* 74, 1168–1183
- Gulley, J.E., Hone, D., Scalapino, D.J. and Silbernagel, B.G. (1970) *Phys. Rev. (B)* 1, 1020–1030
- Gorter, C.J. and Van Vleck, J.H. (1947) *Phys. Rev.* 72, 1128–1129
- Anderson, P.W. and Weiss, P.R. (1953) *Rev. Mod. Phys.* 25, 269–276
- Judeikis, H.S. (1964) *J. Appl. Phys.* 35, 2615–2617
- Shia, L. and Kokoszka, G. (1974) *J. Chem. Phys.* 60, 1101–1105
- Smith, T.D. and Pilbrow, J.R. (1974) *Coord. Chem. Rev.* 13, 173–278
- Kohn, R. and Larsen, B. (1972) *Acta Chem. Scand.* 26, 2455–2468
- Kohn, R. (1972) *Pure Appl. Chem.* 42, 371–397
- Deiana, S., Erre, L., Micera, G., Piu, P. and Gessa, C. (1980) *Inorg. Chim. Acta* 46, 249–253
- Deiana, S., Micera, G., Muggioli, G., Gessa, C. and Pusino, A. (1983) *Colloids Sur.* 6, 17–25
- Havens, J.R. and Koenig, J.L. (1983) *Appl. Spectros.* 37, 226–249
- Andrew, E.R., Bryant, D.J. and Cashell, E.M. (1980) *Chem. Phys. Lett.* 69, 551–554
- Alemany, L.B., Grant, D.M., Pugmire, R.J., Alger, T.D. and Zilm, K.W. (1983) *J. Am. Chem. Soc.* 105, 2133–2141
- Alemany, L.B., Grant, D.M., Pugmire, R.J., Alger, T.D. and Zilm, K.W. (1983) *J. Am. Chem. Soc.* 105, 2142–2147
- Velichko, V.V. and Gusev, A.Y. (1976) *Sov. Phys. J. Eng. Tranl.* 1976, 1200–1201